arXiv:1610.03815v2 [cond-mat.mes-hall] 27 Oct 2016

Electronic structure of graphene: (nearly) free electrons bands vs. tight-binding bands

E. Kogan[1,*] and V. M. Silkin[2,†]

[1] *Jack and Pearl Resnick Institute, Department of Physics, Bar-Ilan University, Ramat-Gan 52900, Israel*
[2] *Donostia International Physics Center (DIPC), Paseo de Manuel Lardizabal 4, E-20018 San Sebastian/Donostia, Spain, Departamento de Física de Materiales, Facultad de Ciencias Químicas, UPV/EHU, Apartado 1072, E-20080 San Sebastian/Donostia, Spain IKERBASQUE, Basque Foundation for Science, 48011 Bilbao, Spain*

(Dated: October 31, 2016)

In our previous paper (Phys. Rev. B **89**, 165430 (2014)) we have found that in graphene, in distinction to the four occupied bands, which can be described by the simple tight-binding model (TBM) with four atomic orbitals per atom, the two lowest lying at the Γ-point unoccupied bands (one of them of a σ type and the other of a π type) can not be described by such model. In the present work we suggest a minimalistic model for these two bands, based on (nearly) free electrons model (FEM), which correctly describes the symmetry of these bands, their dispersion law and their localization with respect to the graphene plane.

PACS numbers: 73.22.Pr

I. INTRODUCTION

In the course of the study of graphite and a graphite monolayer, called graphene, understanding of the symmetries of the electron dispersion law in graphene was of crucial importance. Actually, the symmetry classification of the energy bands in graphene was presented nearly 60 years ago by Lomer in his seminal paper[1]. Later the subject was analyzed by Slonczewski and Weiss[2], Dresselhaus and Dresselhaus[3], Bassani and Parravicini[4], Malard et al[5], Manes[6] and others.

In our previous publication[7] we compared the classification of the electron bands in graphene, obtained by group theory algebra in the framework of a tight-binding model (TBM), with that calculated in a density-functional-theory (DFT) local-density approximation framework. Identification in the DFT band structure of all eight energy bands (four valence and four conduction bands) corresponding to the TBM-derived energy bands was performed and the corresponding analysis was presented. The four occupied (three σ -like and one π -like) and three unoccupied (two σ -like and one π -like) bands given by the DFT closely correspond to those predicted by the TBM, both by their symmetry and their dispersion law. However, the two lowest lying at the Γ-point unoccupied bands (one of them of a σ -like type and the other of a π-like one), were found to be not of the TBM type in accord with the earlier publications[8–11].

In Fig. 1 we reproduce the results of the band structure calculations with symmetry labelling of the occupied and the lowest lying unoccupied bands. The TBM bands are plotted in solid lines, σ non-TBM band - in long dashed, π non-TBM band - in dotted line.

To understand the symmetry classification of the bands one should remember that the group of wave vector $\mathbf{k}$ at the Γ point is D_{6h}; at the K point – D_{3h}; at the point M – D_{2h}. The group of wave vector $\mathbf{k}$ at each of the lines constituting triangle $\Gamma - K - M$ is C_{2v}.[14,15]

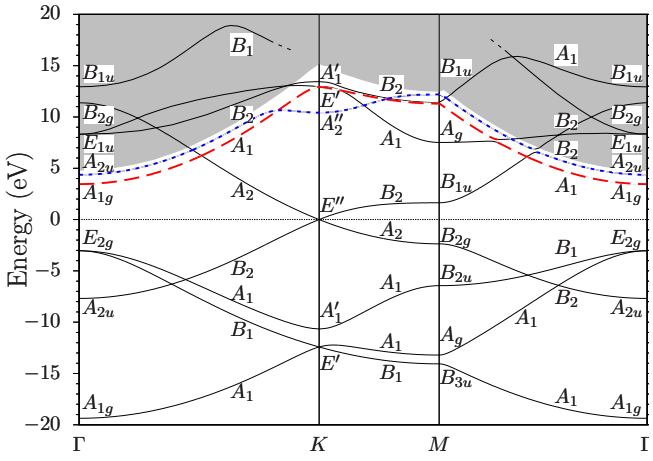

FIG. 1: (color online) Graphene band structure. The dotted line shows the Fermi energy. The grey area corresponds to the vacuum continuum states. The non-TBM bands of our interest are plotted with long-dashed (red) and short-dashed (blue) lines. The upper bands merge into scattering resonances of graphene[12,13], which is schematically shown with dashed (black) endings of lines.

Representations of the groups can be found in the book by Landau and Lifshitz[16]. Honeycomb lattice and its Brillouine zone with the symmetry points are presented on Fig. 2. One of rotations U_2 for the D_{6h} group is about the direction $\Gamma - K$. Rotation C_2^z for the D_{2h} group is about the normal to graphene plane, rotation C_2^x - about the $\Gamma - M$ line. Reflection σ_v for the C_{2v} groups is relative to the plane of graphene. The mathematical details of the symmetry analysis in TBM are presented in Section III.

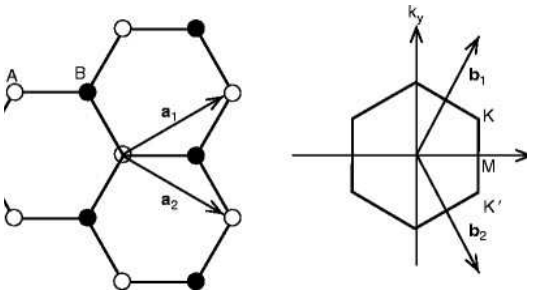

FIG. 2: Honeycomb lattice and its Brillouin zone.

II. FEM BANDS

The difference between the TBM and non-TBM states is evident from the Figures in our previous publication[7] presenting electron density. The former are localized in the vicinity of graphene plane within a distance of the order of graphene lattice constant a. The latter are localized within a distance μa, where $\mu \gg 1$. It means that while calculating the dispersion law with its typical energy scale $\hbar^2/ma^2 \sim 1$ eV, for the non-TBM bands in zero order approximation with respect to parameter $1/\mu$ we can ignore the z dependence of the wave functions. In addition, when looking on Fig. 1 one notices that the dispersion of the two non-TBM bands follow very closely the continuum bottom lines, which present the dispersion law of the free electrons, staying below them.

Hence we can formulate a minimalistic model for the non-TBM bands by considering them as (nearly) free electrons model (FEM) bands, more specifically by presenting their wave functions in the factorised form

$$\psi_{\mathbf{k}}(x,y,z) = f_{\mathbf{k}}(z)\phi_{\mathbf{k}}(x,y), \tag{1}$$

where $\phi_{\mathbf{k}}(x,y)$ are (nearly) free electron wave functions corresponding to the continuum bottom, and the functions $f(z)$ are determined by the boundary conditions

$$\lim_{z\to\pm\infty} f_{\mathbf{k}}(z)) = 0. \tag{2}$$

For the σ band $f(z)$ is an even function, and for the π band – an odd one. The multiplier $f(z)$ would give a first order with respect to parameter $1/\mu$ negative correction to the dispersion of the FEM bands, putting them slightly below the continuum bottom. However, for the symmetry analysis presented below, this multiplier is irrelevant, apart from the fact of its parity, the former distinguishing between σ and π band.

According to the nearly-free-electron model, the wave functions of the states inside the Brillouin zone are just plane waves. On the boundaries of the zone they are combinations of small number of plane waves[18]. Thus, on the lines $\Gamma-K$ and $\Gamma-M$ $\phi_{\mathbf{k}}(x,y) = e^{i\mathbf{k}\cdot\mathbf{r}}$; on the line $K-M$, $\phi_{\mathbf{k}}(x,y)$ is an arbitrary linear combinations of two plane waves: $e^{i\mathbf{k}\cdot\mathbf{r}}$ and the other one, corresponding to the equivalent point on the opposite edge of the hexagon, forming the boundary of the Brillouin zone; at the point K, $\phi_{\mathbf{K}}(x,y)$ is a linear combination of three plane waves $e^{i\mathbf{K}_1\cdot\mathbf{r}}, e^{i\mathbf{K}_2\cdot\mathbf{r}}, e^{i\mathbf{K}_3\cdot\mathbf{r}}$ corresponding to the three equivalent vertices of the hexagon $\mathbf{K}_{1,2,3}$.

Our assumption allows to derive the symmetry realized by each of the two bands from the symmetry of plane waves with respect to rotations and reflections in the plane (and the symmetry of the function $f(z)$ with respect to reflection in the $z=0$ plane).

Thus we immediately obtain that at the point Γ, the σ band realizes representation A_{1g}, and the π – representation A_{2u}. At the lines $\Gamma-K$ and $\Gamma-M$, the σ band realizes representation A_1, and the π – representation B_2.

At the line $K-M$ the function $f(z)\times$ (sum of the exponents) realizes A_1 representation of C_{2v} for even $f(z)$, and B_2 representation for odd $f(z)$; the function $f(z)\times$ (difference of the exponents) realizes B_1 representation for even $f(z)$, and A_2 representation for odd $f(z)$. One can expect that the two bands considered correspond to symmetric combinations of the plane waves.

At the point M the function $f(z)\times$ (sum of the exponents) realizes A_g representation of D_{2h} for even $f(z)$, and B_{1u} representation for odd $f(z)$; the function $f(z)\times$ (difference of the exponents) realizes B_{3u} representation of D_{2h} for even $f(z)$, and B_{2g} representation for odd $f(z)$. Again, one can expect that the two bands considered would correspond to symmetric combinations of the plane waves.

To expand the representation realized by the plane waves at the point K we may use equation[16]

$$a^{(\alpha)} = \frac{1}{g}\sum_G \chi(G)\chi^{\alpha}(G)^*, \tag{3}$$

where $a^{(\alpha)}$ shows how many times an irreducible representation α of the group (in our case D_{3h}) occurs in the expansion, g is the number of elements in the group, G is an arbitrary element of the group, $\chi(G)$ is the character of the element in the origional representation, and $\chi^{\alpha}(G)$ is the character of the element in the irreducible representation α.

Taking into account the table of the characters of the irreducible representations of the group D_{3h} we get that at the point K the functions $f(z)\times\left\{e^{i\mathbf{K}_1\cdot\mathbf{r}}, e^{i\mathbf{K}_2\cdot\mathbf{r}}, e^{i\mathbf{K}_3\cdot\mathbf{r}}\right\}$ realize $A_1' + E'$ representation of D_{3h} for even $f(z)$, and $A_2'' + E''$ representation for odd $f(z)$[19]. More specifically, according to the FEM[18], in the vicinity of the K point there are 3 σ and 3 π bands which are linear combinations of the 3 plane waves, corresponding to the equivalent vertices of the Brillouine zone hexagon (multiplied by the appropriate $f(z)$ functions. Judging by the band structure presented on Fig. 1, in each case two upper bands are high in the continuum, and the lower one is below the continuum bottom.

The FEM σ states in the vicinity of the K point are hybridized with the TBM σ states. Thus the E' representation of the unoccupied bands is realized by the states of both types[7,19] (see also the next Section).

On the other hand, the FEM π states in the vicinity of the K point have no TBM counterparts, to hybridize

with. However, the lower FEM band in the vicinity of the K point is repelled by the upper bands. (Formally, the upper bands exist all over the Brillouine zone, but they come close to the lower one only in the vicinity of the K point.) This explains why the FEM π band deviates from the bottom of the continuum there.

III. TBM BANDS

The first attempt to apply the TBM to the calculation of the electrons dispersion law in graphene (graphite) was done already in 1935 by F. Hund and B. Mrowka[20].

Here we want to expand the symmetry analysis in the framework of the TBM from our previous publications[7,19]. We look for the solution of the Schrödinger equation as a linear combination of the functions

$$\psi^j_{\beta;\mathbf{k}} = \sum_{\mathbf{R}_j} e^{i\mathbf{k}\cdot\mathbf{R}_j}\psi_\beta\left(\mathbf{r}-\mathbf{R}_j\right), \tag{4}$$

where ψ_β are atomic orbitals, $j = A, B$ labels the sublattices, and $\mathbf{R}_j$ is the radius vector of an atom in the sublattice j. Our TBM space includes four atomic orbitals: $|s, p>$. (Notice that we assume only symmetry of the basis functions with respect to rotations and reflections; the question how these functions are related to the atomic functions of the isolated carbon atom is irrelevant.)

The Hamiltonian of graphene being symmetric with respect to reflection in the graphene plane, the bands built from the $|p_z>$ orbitals decouple from those built from the $|s, p_x, p_y>$ orbitals. The former are odd with respect to reflection, the latter are even. In other words, the former form π bands, and the latter form σ bands.

A symmetry transformation of the functions $\psi^j_{\beta;\mathbf{k}}$ is a direct product of two transformations: the transformation of the sub-lattice functions $\phi^{A,B}_{\mathbf{k}}$, where

$$\phi^j_{\mathbf{k}} = \sum_{\mathbf{R}_j} e^{i\mathbf{k}\cdot\mathbf{R}_j}, \tag{5}$$

and the transformation of the orbitals ψ_β. Thus the representations realized by the functions (4) will be the direct product of two representations.

A. Γ - point

Let us start from the most symmetrical point Γ. The functions $\phi^{A,B}_{\mathbf{0}}$ realize $A_{1g} + B_{1u}$ representation of the group D_{6h}. The orbital $|s>$ realizes A_{1g} representation of the group, $|p_z>$ realizes A_{2u} representation, the orbitals $|p_x, p_y>$ realize E_{1u} representation. The identitity

$$(A_{1g} + B_{1u}) \times A_{1g} = A_{1g} + B_{1u} \tag{6}$$

specifies the two σ bands constructed from $|s>$ orbitals; the identity

$$(A_{1g} + B_{1u}) \times A_{2u} = A_{2u} + B_{2g} \tag{7}$$

specifies the two π bands constructed from $|p_z>$ orbitals; the identity

$$(A_{1g} + B_{1u}) \times E_{1u} = E_{1u} + E_{2g} \tag{8}$$

shows that there are two merging points of the σ bands constructed from $|p_{x,y}>$ orbitals.

Eqs. (6) - (8) explain why the band A lies below the corresponding B band, and the degeneracy of the bands corresponding to E_1 representation occurs below of those corresponding to the E_2 representation. In fact, the symmetry of the band(s) with respect to exchange of the lattice sites (the higher symmetry corresponding to the lower band[18]) can be deduced from the symmetry of the representation realized by $\phi^j_{\mathbf{k}}$.

B. K - point

Now consider the point K. The functions $\phi^{A,B}_{\mathbf{K}}$ realize E' representation of the group D_{3h}. The orbitals $|s>$ and $|p_z>$ realize A'_1 and A''_2 representations respectively, the orbitals $|p_x, p_y>$ realize E' representation. The product of the representations is expanded as

$$\begin{array}{l} E' \times A'_1 = E' \\ E' \times A''_2 = E'' \\ E' \times E' = A'_1 + E' + A'_2. \end{array} \tag{9}$$

(Notice that $A'_1 + E'$ is the symmetric product of the representation on itself (including, of course, the absolutely symmetric representation A_1 and A'_2 is the antisymmetric product[16].) Taking into account these identities, we obtain a band realizing A'_1 representation and that realizing A'_2 representation, constructed from $|p_x, p_y>$ orbitals, two merging points realizing E' representations, each of them constructed from $|s, p_x, p_y>$ orbitals and the merging point realizing E'' representation, constructed from $|p_z>$ orbitals.

On Figs. 3 -5 we present the results of the calculations of the wave functions of the non degenerate bands at the point K. The wave functions of the σ bands are plotted at the plane $z = 0$. For the π band, the wave function is identically equal to zero at the $z = 0$ plane, so we plotted the wave function at the plane $z = 1$ a.u. All the Figures are consistent with the assignments made in Fig. 1.

In our previous publication[19] we presented simple TBM interpretation of the degeneracy of the π bands at the point K (E'' representation). The general TBM Hamiltonian for the π bands is

$$H = -\begin{pmatrix} E_p + \sum_{\mathbf{a}} t'(\mathbf{a}) e^{i\mathbf{k}\cdot\mathbf{a}} & \sum_{\mathbf{a}} t(\mathbf{a}+\delta) e^{i\mathbf{k}\cdot(\mathbf{a}+\delta)} \\ \sum_{\mathbf{a}} t^*(\mathbf{a}+\delta) e^{-i\mathbf{k}\cdot(\mathbf{a}+\delta)} & E_p + \sum_{\mathbf{a}} t'(\mathbf{a}) e^{i\mathbf{k}\cdot\mathbf{a}} \end{pmatrix}, \tag{10}$$

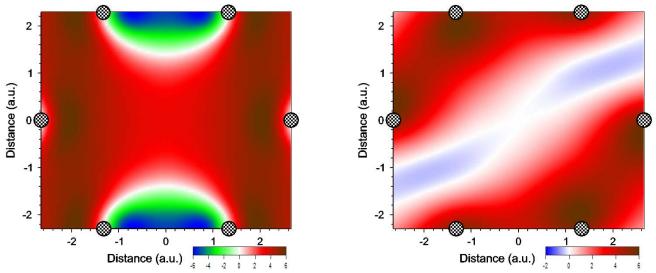

FIG. 3: (color online) Real (left) and imaginary (right) parts of the wave function (in arbitrary units) at the $z = 0$ plane for the third lowest band at K point.

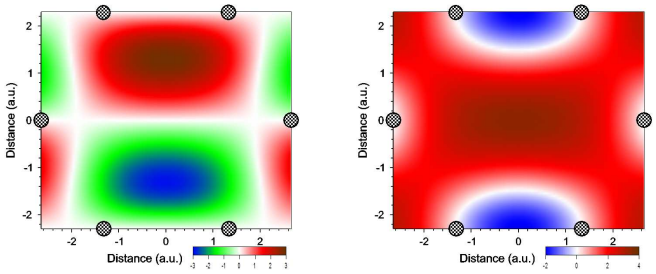

FIG. 4: (color online) Real (left) and imaginary (right) parts of the wave function (in arbitrary units) at the $z = 1$ a.u. plane for the sixth lowest band at K point.

where E_p is the energy of an isolated $|p_z>$ orbital, $\mathbf{a}$ is an arbitrary lattice vector. The structure of graphene can be seen as a triangular lattice with a basis of two atoms per unit cell, displaced from each other by any one (fixed) vector δ connecting two sites of different sublattices. From Ref.[17] we get that $\mathbf{a}$ is a linear combination of $\mathbf{a}_1 = \frac{a}{2}\left(3, \sqrt{3}\right)$, $\mathbf{a}_2 = \frac{a}{2}\left(3, -\sqrt{3}\right)$ and δ can be chosen as $\delta = -a\,(1, 0)$. Also $K = \frac{2\pi}{3a}\left(1, \frac{1}{\sqrt{3}}\right)$.

Consider, for example, three terms in the sum $\sum_{\mathbf{a}} t(\mathbf{a}+\delta)e^{i\mathbf{k}\cdot(\mathbf{a}+\delta)}$ corresponding to hopping between the nearest neighbours. The hopping integral $t(\mathbf{a}+\delta)$ is the same for all three terms; the multiplier $e^{i\mathbf{k}\cdot(\mathbf{a}+\delta)}$ takes three values: $1, e^{2\pi i/3}, e^{-2\pi i/3}$, $\epsilon = e^{2\pi i/3}$. Hence, due to the identity $1 + e^{2\pi i/3} + e^{-2\pi i/3} = 0$, the non-diagonal terms in the Hamiltonian (10) disappear; hence degeneracy of the bands.

Similar interpretation can be supplied for the degeneracy of the σ bands at the K point. The reasoning from the previous paragraph can be repeated verbatim for the E' representation realized by ψ_s^A and ψ_s^B functions. The TBM analysis of the representations realized by $\psi_{p_{x,y}}^{A,B}$ functions is a bit more complicated.

Let us start defining a convenient for our purpose basis for the E representation of the group C_{3v} realized by $|p_{x,y}>$ orbitals:

$$
\begin{aligned}
|p_L> &= |p_x> + \epsilon\hat{T}|p_x> + \epsilon^2\hat{T}^2|p_x> \\
|p_R> &= |p_x> + \epsilon^2\hat{T}|p_x> + \epsilon\hat{T}^2|p_x>,
\end{aligned}
\tag{11}
$$

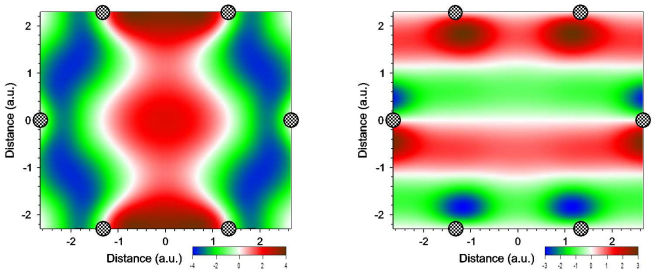

FIG. 5: (color online) Real (left) and imaginary (right) parts of the wave function (in arbitrary units) at the $z = 0$ plane for the ninth lowest band at K point.

where $\hat{T}$ is an operator of rotation by the angle $2\pi/3$. If we graphically present $|p_x>$ orbital by a line in the x-direction, then the basis vectors can be presented as two stars.

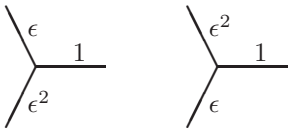

It is obvious that rotation of each basis vector by $2\pi/3$ just multiplies it by ϵ (ϵ^2).

Returning to our original representation we chose the basis vectors as

$$
\begin{aligned}
\psi_1 \equiv \psi_L^A &= \textstyle\sum_{\mathbf{R}_A} e^{i\mathbf{K}\cdot\mathbf{R}_A}|p_L>_{\mathbf{R}_A} \\
\psi_2 \equiv \psi_R^A &= \textstyle\sum_{\mathbf{R}_A} e^{i\mathbf{k}\cdot\mathbf{R}_A}|p_R>_{\mathbf{R}_A} \\
\psi_3 \equiv \psi_L^B &= \textstyle\sum_{\mathbf{R}_B} e^{i\mathbf{k}\cdot\mathbf{R}_B}|p_R>_{\mathbf{R}_B} \\
\psi_4 \equiv \psi_R^B &= \textstyle\sum_{\mathbf{R}_B} e^{i\mathbf{k}\cdot\mathbf{R}_B}|p_R>_{\mathbf{R}_B},
\end{aligned}
\tag{12}
$$

where $|\cdots>_{\mathbf{R}}$ means an orbital centered at the site $\mathbf{R}$. The Hamiltonian matrix in such basis has the form

$$
H = \begin{pmatrix} 0 & \dots & 0 & \dots \\ \dots & 0 & \dots & 0 \\ 0 & \dots & 0 & \dots \\ \dots & 0 & \dots & 0 \end{pmatrix},
\tag{13}
$$

where we have shifted energy to $H_{11} + E_p$ (E_p is the energy of an isolated $|p>$ orbital). The elements indicated by three dots are of no interest to us. The origin of zeros on the diagonal of the matrix is obvious. To understand presence of non-diagonal zeros (in a chosen basis) consider, for example, the three terms in the H_{13} matrix element corresponding to hopping between the nearest neighbours. They can be graphically presented as

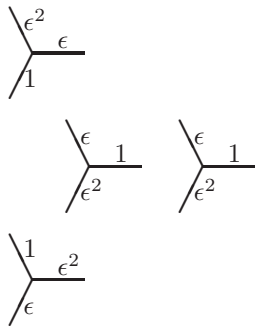

Again, the identity $1 + e^{2\pi i/3} + e^{-2\pi i/3} = 0$ leads to the disappearance of the matrix element. The structure of the matrix (13) shows that its eigenvalues can be grouped into pairs with the the same modulus and the opposite signs. On the other hand, this structure shows that the product of all eigenvalues is equal to zero. Hence degeneracy of the bands at the energy 0 (that is at the energy $H_{11} + E_p$).

C. M - point

Finally consider the point M. The functions ψ^j_{M} realize $A_g + B_{3u}$ representation of the group D_{2h}. The orbitals $|s>$, $|p_z>$, $|p_x>$ and $|p_y>$ realize A_g, B_{1u}, B_{3u} and B_{2u} representations respectively. Thus the identity

$$(A_g + B_{3u}) \times B_{1u} = B_{1u} + B_{2g} \tag{14}$$

shows the symmetry of the two π bands at the point M; the identity

$$(A_g + B_{3u}) \times B_{2u} = B_{2u} + B_{1g} \tag{15}$$

shows the symmetry of the two σ bands constructed from $|p_y>$ orbitals, and the identities

$$\begin{array}{l}(A_g + B_{3u}) \times B_{3u} = B_{3u} + A_g \\ (A_g + B_{3u}) \times A_g = A_g + B_{3u}\end{array} \tag{16}$$

show that there are two A_g and two B_{3u} bands constructed from $|p_x>$ and $|s>$ orbitals.

From analyzing the TBM[17] we come to the conclusion that the band B_{1u} lies above the band B_{2g}. From Eq. (16) we come to the conclusion that, if overlapping between $|p_x>$ orbitals is stronger than that between $|s>$ orbitals, the lowest band at the point M realizes B_{3u} reprezentation.

On Figs. 6 -10 we present the results of the calculations of the wave functions of the occupied and the lowest unoccupied bands at the point M. The wave functions of the σ bands are plotted at the plane $z = 0$. For the π bands, the wave function is identically equal to zero at the $z = 0$ plane, so we plotted the wave function at the plane $z = 1$ a.u.

For the lowest (at the point M) band the wave function is equal to zero along the y - axis, which corresponds to the representation B_{3u}. (Because the wave function is antisymmetric with respect to reflection, it should be equal to zero at the axis of reflection.) The wave function of the next band is different from zero everywhere at the plane, which is consistent with the representation A_g. The wave function of the third band is equal to zero at the x -axis, which corresponds to the representation B_{2u}.

For the forth band the wave function is equal to zero along the y - axis, which corresponds to the representation B_{2g}. The wave function of the first unoccupied band is different from zero everywhere at the plane $z = 1$ a.u., which is consistent with the representation B_{1u}.

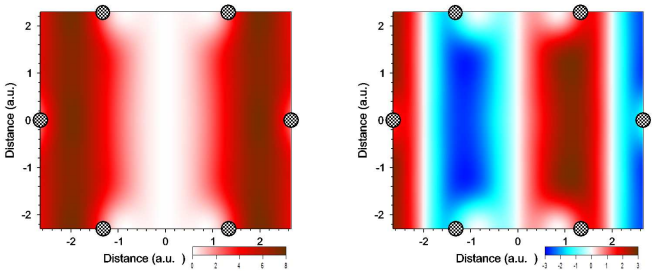

FIG. 6: (color online) Real (left) and imaginary (right) parts of the wave function (in arbitrary units) at the $z = 0$ plane for the lowest band at M point.

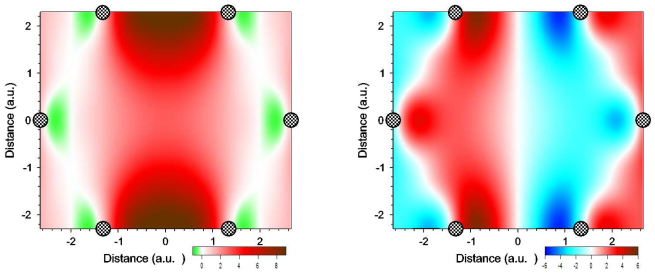

FIG. 7: (color online) Real (left) and imaginary (right) parts of the wave function (in arbitrary units) at the $z = 0$ plane for the second lowest band at M point.

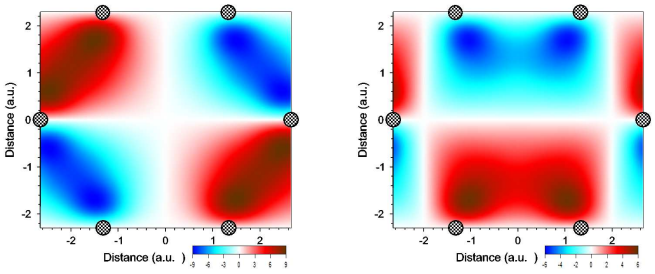

FIG. 8: (color online) Real (left) and imaginary (right) parts of the wave function (in arbitrary units) at the $z = 0$ plane for the third lowest band at M point.

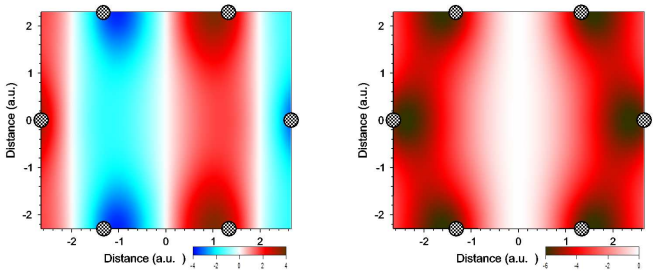

FIG. 9: (color online) Real (left) and imaginary (right) parts of the wave function (in arbitrary units) at the $z = 1$ a.u. plane for the forth lowest band at M point.

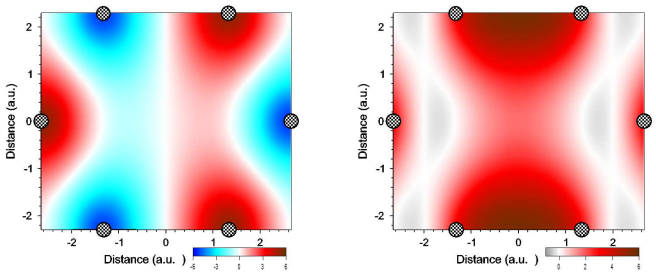

FIG. 10: (color online) Real (left) and imaginary (right) parts of the wave function (in arbitrary units) at the $z = 1$ a.u. plane for the fifth lowest band at M point.

D. $\Gamma - K - M$ - lines

The symmetry of the band(s) at the symmetry point determines the symmetry of the band(s) at the symmetry lines containing this point[15,16]. At the line $\Gamma - K - M$ the functions $\phi_{\mathbf{k}}^{A,B}$ realize $A_1 + B_1$ representation of the group C_{2v}. The orbital $|p_z>$ realizes B_2 representation. From the identities $B_2 \times A_1 = B_2$, $B_2 \times B_1 = A_2$ we come to the conclusion that the lower band should realize B_2 representation. At the line $\Gamma - M$ the functions $\phi_{\mathbf{k}}^{A,B}$ realize twice A_1 representation of the group C_{2v}. The orbital $|p_z>$ generalizes B_2 representation. From the identity $B_2 \times A_1 = B_2$ we obtain that both π bands realize B_2 representation.

Acknowledgments

The authors are grateful for the useful discussions to P. D. Esquinazi, M. I. Katsnelson, A. I. Lichtenstein, V. U. Nazarov, N. S. Pavlov, O. Rader, L. M. Sandratskii, and V. Varykhalov. They are also grateful to P. D. Esquinazi for bringing to their attention Ref.[20].

C_{2v}		E	C_2	σ_v	σ_v'
	D_2	E	C_2^z	C_2^y	C_2^x
$A_1; z$	A	1	1	1	1
$B_2; y$	$B_3; x$	1	−1	−1	1
A_2	$B_1; z$	1	1	−1	−1
$B_1; x$	$B_2; y$	1	−1	1	−1

TABLE I: Character table for irreducible representations of C_{2v} and D_2 point groups

D_6		E	C_2	$2C_3$	$2C_6$	$3U_2$	$3U_2'$
	D_{3h}	E	σ	$2C_3$	$2S_3$	$3U_2$	$3\sigma_v$
A_1	A_1'	1	1	1	1	1	1
A_2	A_2'	1	1	1	1	−1	−1
B_1	A_1''	1	−1	1	−1	1	−1
B_2	A_2''	1	−1	1	−1	−1	1
E_2	E'	2	2	−1	−1	0	0
E_1	E''	2	−2	−1	1	0	0

TABLE II: Character table for irreducible representations of D_6 and D_{3h} point groups

IV. APPENDIX

For convenience of the reader in we reproduce character tables for the groups used in the paper[16] (Tables I and II).

The characters of the groups D_{2h} and D_{6h} are obtained using the relations $D_{2h} = D_2 \times C_i$ and $D_{6h} = D_6 \times C_i$, where C_i is the inversion group.

* Electronic address: Eugene.Kogan@biu.ac.il
† Electronic address: vyacheslav.silkin@ehu.es

[1] W. M. Lomer, Proc. R. Soc. London, Ser. A **227**, 330 (1955).
[2] J. C. Slonczewski and P. R. Weiss, Phys. Rev. **109**, 272 (1958).
[3] G. Dresselhaus and M. S. Dresselhaus, Phys. Rev. **140**, A401 (1965).
[4] F. Bassani and G. Pastori Parravicini, Nuovo Cimento B **50**, 95 (1967).
[5] L. M. Malard, M. H. D. Guimaraes, D. L. Mafra, M. S. C. Mazzoni, and A. Jorio, Phys. Rev. B **79**, 125426 (2009).
[6] J. L. Manes, Phys. Rev. B **85**, 155118 (2012).
[7] E. Kogan, V. U. Nazarov, V. M. Silkin, and M. Kaveh, Phys. Rev. B **89**, 165430 (2014).
[8] M. Posternak, A. Baldereschi, A. J. Freeman, E. Wimmer, and M. Weinert, Phys. Rev. Lett. **50**, 761 (1983).
[9] M. Posternak, A. Baldereschi, A. J. Freeman, and E. Wimmer, Phys. Rev. Lett. **52**, 863 (1984).
[10] T. O. Wehling, I. Grigorenko, A. I. Lichtenstein, and A. V. Balatsky, Phys. Rev. Lett. **101**, 216803 (2008).
[11] V. M. Silkin, J. Zhao, F. Guinea, E. V. Chulkov, P. M. Echenique, and H. Petek, Phys. Rev. B **80**, 121408(R) (2009).
[12] V. U. Nazarov, E. E. Krasovskii, and V. M. Silkin, Phys. Rev. B, **87**, 041405(R) (2013).
[13] F. Wicki, J.-N. Longchamp, T. Latychevskaia, C. Escher, and H.-W. Fink, Phys. Rev. B **94**, 075424 (2016).
[14] M. S. Dresselhaus, G. Dresselhaus, A. Jorio, *Group theory: Application to the physics of condenced matter*, (Springer-Verlag Berlin Heidelberg, 2008).
[15] C. Thomsen, S. Reich, J. Maultzsch, *Carbon Nanotubes: Basic Concepts and Physical Properties*, (Wiley Online Library, 2004 WILEY-VCH Verlag GmbH).
[16] L. D. Landau and E. M. Lifshitz, *Landau and Lifshitz Course of Theoretical Physics: Vol. 3 Quantum Mechanics*, (Pergamon Press, 1991).
[17] A. H. Castro Neto, F. Guinea, N. M. R. Peres, K. S. Novoselov and A. K. Geim, Rev. Mod. Phys. **81**, 109 (2009).
[18] C. Kittel, *Quantum Theory of Solids*, (John Willey & Sons. Inc., New York - London, 1963).
[19] E. Kogan and V. U. Nazarov, Phys. Rev. B **85**, 115418 (2012)
[20] F. Hund and B. Mrowka, Sachs. Akad. Wiss., Leipzig **87**, 325 (1935).